The Astrophysical Journal, 823:3 (8pp), 2016 May 20 doi:10.3847/0004-637X/823/1/3

A GLOBAL MAGNETIC TOPOLOGY MODEL FOR MAGNETIC CLOUDS. IV.

M. A. Hidalgo
Departamento de Física y Matemáticas, Universidad de Alcalá, Spain; miguel.hidalgo@uah.es
Received 2015 October 15; accepted 2016 March 15; published 2016 May 13

ABSTRACT

In the first paper of this series, we introduced a global topology model for the study of magnetic clouds (MCs), fitting it to the experimental magnetic field components and obtaining, for example, the orientation of the axis of the MCs in the interplanetary medium. In the third paper, we extended the model to include theoretical hydrostatic plasma pressure, also incorporating it in the fitting procedure. The present work is complementary to the previous ones, now incorporating the proton current density as deduced from the continuity equation. In particular, we are interested in the component of the proton current density parallel to the magnetic field lines of the MC, $\boldsymbol{j}\|$, because the perpendicular component is expected to have information similar to the plasma pressure. Under all of these conditions, our fitting procedure now involves simultaneous analysis of the three components of the magnetic field, the trace of the plasma pressure, and the parallel proton current density. This provides us with more information about the physical mechanisms taking place inside MCs, thus helping us to understand the propagation and evolution of these structures in the interplanetary medium.

Key words: solar–terrestrial relations – solar wind – Sun: coronal mass ejections (CMEs) – Sun: heliosphere – Sun: magnetic fields

1. INTRODUCTION

It is now firmly established that coronal mass ejections (CMEs), which are huge eruptions of solar plasma and magnetic field, are associated with specific signatures in the heliospheric, commonly called interplanetary CMEs (ICMEs; e.g., Webb et al. 2000). About one-third of ICMEs feature smooth rotation of the magnetic field, a high magnetic field strength, and low plasma beta which is indicative of the magnetic flux-rope configuration (Burlaga et al. 1981). Such organized structures are referred to as magnetic clouds (MCs).

Although only a fraction of ICMEs show MC signatures, it is the consensus that all CMEs initially have a flux-rope structure (Vourlidas et al. 2012); however, in-situ observations often do not show such structures due to deformation during their evolution in the interplanetary medium, or due to large impact parameters. Thus, not all ICMEs are expected to show such signatures (Gosling 1990; Jian et al. 2006; Kilpua et al. 2011). Therefore, although there are several models in the literature for the analysis of the magnetic field in MCs (briefly summarize below) and their physics is now relatively well understood, deeper knowledge of the physical mechanisms inside them is still an open question, mainly because the behavior of the plasma is not yet well understood.

Thus, from the theoretical point of view, the main purpose of studying the MC phenomenon is to develop a model, either analytical or numerical, that allows us to determine its physical parameters from experimental measurements, providing a global view of their properties. We have to bear in mind that in-situ observations typically only provide a single cut through a flux-rope structure.

However, until now, most of the models in the literature have only analyzed the magnetic field topology of the MCs. Hence, it is necessary to involve the behavior of the plasma inside them if we want to advance our understanding of the phenomenon. In fact, some efforts in this direction have already been made in recent years (Cid et al. 2002; Hidalgo 2014).

In this last sense, most MC models in the literature assume a force-free character, which implicitly implies, for example, that the plasma pressure is constant inside the MC. In addition, this force-free character means that the plasma current density and the magnetic field lines are parallel, i.e., thus fulfilling the equation $\boldsymbol{j} = \alpha \boldsymbol{B}$. Lundquist (1950) found static axially symmetric magnetic field solutions using this restriction in the Maxwell equations and assuming cylindrical geometry. Initially, this approach was used assuming that the parameter α was constant (Burlaga 1988). Later, Goldstein (1983) proposed a non-constant α, which is more appropriate for the study of MCs with $\nabla \times \boldsymbol{B} = \alpha(\boldsymbol{r})\boldsymbol{B}$. However, even this more general configuration of the magnetic field (and plasma current density) leads to the equation $\nabla \boldsymbol{p} = 0$, i.e., the pressure is constant inside the MC time interval. However, through visual inspection, it is clear that the assumption of constant pressure contradicts experimental measurements (Hidalgo 2014). Therefore, the non-force-free character is already accepted as the appropriated scenario for understanding the evolution and propagation of the MCs in the interplanetary medium. Moreover, the numerical and simulation models also support this last idea because they are capable of describing the dynamical processes and mechanisms in the evolution of the MCs, and in some simple cases their interactions (Riley et al. 2001; Hu & Sonnerup 2002; Riley & Crooker 2004).

A crucial problem concerning the analysis of MCs with any model is the choice of the boundaries from experimental data (Hu & Sonnerup 2002; Richardson & Cane 2010; Kilpua et al. 2013). In some cases, boundaries can be determined from the physical parameters obtained from the fitting (Hidalgo et al. 2013). This was one of the main aims of the workshop "Living with a Star Coordinated Data Analysis Workshop: Do all CMEs have flux-rope structure?." One was held in San Diego in 2010 September and the second was held in Alcalá de Henares, Spain in 2011 September ("Flux-Rope Structure of CMEs," Solar Physics, volume 284, 2013 May, Guest Editors: N. Gopalswamy, T. Nieves-Chinchilla, M. A. Hidalgo, J. Zhang and P. Riley). Hence, it is important to bear in mind that a reliable analytical model for studying MCs can also be a feedback tool for establishing their appropriate boundaries. In

this sense, the Grad–Shafranov reconstruction technique provides flux-rope boundaries as the output of the reconstruction (Möstl et al. 2009).

From the experimental point of view, two complementary sources of information can be used: remote sensing observations from spacecraft looking at the Sun's surface, and in-situ measurements typically sampled near 1 au. As we have detailed above, from the theoretical point of view, two approaches are provided in the literature: analytical models and numerical simulations.

The remote sensing techniques provide us with three-dimensional geometrical information on the CME in close proximity to the Sun, helping us to understand of how they eject, evolve, and propagate in the interplanetary medium (especially useful has been the *STEREO* mission; Thernisen et al. 2009).

The present work is a new step in the development of a reliable analytical model for the global magnetic topology of MCs, which began with the three previous works of Hidalgo & Nieves-Chinchilla (2012) and Hidalgo (2013, 2014). The model presented in this paper is the first analytical MC model in the literature that considers the plasma current density and plasma pressure.

The paper is organized as follows. In the next section, Section 2, we provide the expressions for the global topology assumed for the MCs of the magnetic field components, the plasma hydrostatic pressure, and both plasma current density components: perpendicular and parallel to the magnetic field line topology. (As we describe below, we are interested in the parallel component, $\boldsymbol{j}\|$ (Equation (16)), because it provides complementary information to that involved in the plasma pressure.) Section 3 is devoted to explaining the procedure proposed to fit the model to the experimental data. The data used are described in Section 4: we have selected six events which show different shapes in plasma and magnetic field behavior. In Section 5, we discuss and summarize our results.

2. THE MODEL

One of the most important tasks in understanding the physical mechanisms taking place inside MCs when they evolve in the interplanetary medium is to find the relation between their magnetic field and the corresponding plasma. In the literature, the detailed behavior of the plasma associated with the MCs remains an open problem. In fact, we have already noted that Goldstein's model 1983, the Lepping et al. (1997) model, and even all of the models with force-free character cannot explain the plasma pressure variations within the MC because they assume constant pressure. However, since the earliest years, some efforts toward incorporating the plasma behavior for the assumed MC topology have been made, from both the analytical (Osherovich et al. 1993, 1995; Cid et al. 2002) and numerical and/or simulation points of view (for example, Hu & Sonnerup 2002).

Here, our starting point will be the analytical global model we began to develop four years ago. When choosing the appropriate intrinsic coordinates for the MCs' topology, we assumed a toroidal coordinate system where the minus radius of the torus varies along it, as well as some additional assumptions (Hidalgo & Nieves-Chinchilla 2012; Hidalgo 2013, 2014). When solving the Maxwell equations for the magnetic field, and the force and continuity equations, we determine the analytical expressions for the magnetic field vector, $\boldsymbol{B} = B_\phi \boldsymbol{e}_\phi + B_\psi \boldsymbol{e}_\psi + B_\eta \boldsymbol{e}_\eta$, the plasma pressure, and the plasma current density, given by

$$\begin{aligned} \boldsymbol{j} \;=\; & j_\varphi \boldsymbol{e}_\varphi + j_\psi \boldsymbol{e}_\psi + j_\eta \boldsymbol{e}_\eta = (j_\varphi^e + j_\varphi^p)\boldsymbol{e}_\varphi \\ & + (j_\psi^e + j_\psi^p)\boldsymbol{e}_\psi + (j_\eta^e + j_\eta^p)\boldsymbol{e}_\eta \end{aligned} \quad , \tag{1}$$

where $\boldsymbol{j}^e$ and $\boldsymbol{j}^p$ correspond to the electron and proton current densities, respectively.

Then, for the poloidal component of the magnetic field, we have

$$B_\varphi = B_\varphi^0(\psi)\cos(\varphi) - \mu_0 j_\psi r \cosh(-\rho_0\eta + f(\psi)) \tag{2}$$

with

$$B_\varphi^0(\psi) = B_{0\varphi}^0 \sin\left(\frac{\psi}{2}\right), \tag{3}$$

where $B_{0\varphi}^0$ depends on r, and linearly on time, i.e., $B_\varphi^0 \approx (t_0 - t)$.

The auxiliary function $f(\psi)$ allows us to represent different MC topologies (in future publications, we will explore this possibility of the model). In the present case, as a first approach, we assume the simpler dependence

$$f(\psi) = C \sin\left(\frac{\psi}{2}\right) \tag{4}$$

with C being an adjustable constant.

The axial magnetic field component is given by

$$B_\psi = B_\psi^0(\psi) + \mu_0 j_\varphi r \cosh(-\rho_0\eta + f(\psi)), \tag{5}$$

where $B_\psi^0(\psi)$ is the axial magnetic field at the axis of the torus,

$$B_\psi^0(\psi) = B_{0\psi}^0 \left|\cos\left(\frac{\psi}{2}\right)\right|, \tag{6}$$

where $B_{0\psi}^0$ is approaching being spatially constant, although with a linear time dependence, i.e., $B_\psi^0 \approx (t_0 - t)$.

Finally, for the third component of the magnetic field, we have

$$\begin{aligned} B_\eta \;=\; & -2\cos(\varphi) S \left\{ B_{0\psi}^0 \sin\left(\frac{\psi}{2}\right) + \frac{1}{C}\mu_0 \alpha (t_0 - t)\, r^2 \right. \\ & \left. \times \cosh(-\rho_0\eta + f(\psi)) \right\} \end{aligned} \quad , \tag{7}$$

where the term $S = \sqrt{\sin^2(\psi)}\,/\sin(\psi)$ represents the Heaviside function.

In the following, we will assume neutral plasma, i.e., the densities of the electrons and protons are identical. This is necessary to avoid electrical instabilities within in the magnetic structure, which is consistent with the stability of the MCs over their extended propagation in the interplanetary medium.

In relation to this last assumption, and concerning the continuity equation, we assume stationary conditions at the timescale we are interested in, i.e., that associated with the evolution of the cloud during the passage of the spacecraft through it. This means that we can suppose that $\partial(\rho_e + \rho_p)/\partial t = 0$. Moreover, it will be important to bear in mind that this also implies that the behavior of both current densities inside MCs, those due to protons and electrons, are

similar because $\nabla \cdot \boldsymbol{j} = \nabla \cdot (\boldsymbol{j}^e + \boldsymbol{j}^p) = 0$, i.e., we have

$$\nabla \boldsymbol{j}^p = -\nabla \boldsymbol{j}^e . \quad (8)$$

Hence, under this condition, together with the Maxwell equations for the magnetic field, we can obtain the plasma current density components, given by

$$j_\varphi = \alpha (t_0 - t)\, r \left| \cos\left(\frac{\psi}{2}\right) \right| \quad (9)$$

for the poloidal component, and

$$j_\psi = \lambda (t_0 - t) \sin\left(\frac{\psi}{2}\right) \quad (10)$$

for the axial component. The terms α and λ are parameters of the model that can be obtained from the fitting process.

It is necessary to assume a linear time dependence for the plasma current density (and, then, for the magnetic field and the plasma pressure) for the model to be consistent, and because the magnetic field components of the model are deduced by neglecting the displacement current from the Maxwell–Ampere law. A detailed description of this can be found in Hidalgo (2011).

Eventually, considering the following hypothesis on the kinematics of the plasma inside the MCs, $\frac{d\boldsymbol{v}^e}{dt} = \frac{d\boldsymbol{v}^p}{dt} \approx 0$, we can simplify the force equation as $-\nabla \cdot \overline{\overline{p^t}} + \boldsymbol{j} \times \boldsymbol{B} = 0$, where $\overline{\overline{p^t}} = \overline{\overline{p^e}} + \overline{\overline{p^p}}$ is the total plasma pressure tensor associated with both species inside the cloud. Therefore, we obtain

$$p_\varphi = p_\varphi^0 - 2 j_\psi r \tan(\varphi) \cos(\varphi) S \left\{ B_{0\psi}^0 \sin\left(\frac{\psi}{2}\right) + \frac{1}{C} \mu_0 \alpha (t_0 - t)\, r^2 \cosh(-\rho_0 \eta + f(\psi)) \right\} \quad (11)$$

$$p_\psi = p_\psi^0 + 2\alpha (t_0 - t) B_{0\psi}^0 \rho_0 r \cos(\varphi) \sin^2\left(\frac{\psi}{2}\right) - \frac{4}{C^2} \mu_0 (\alpha (t_0 - t))^2 \rho_0 r^2 \cos(\varphi) \quad (12)$$

$$p_\eta = -(j_\varphi B_\psi^0 - j_\psi B_\varphi^0 \cos(\varphi)) \frac{r}{2} \cos(\varphi) - \frac{\mu_0}{2} (j_\varphi^2 + j_\psi^2) r^2 . \quad (13)$$

p_φ^0 and p_ψ^0 are constant terms. Hence, from Equations (11)–(13), we can calculate the trace of the plasma pressure tensor that we include in the fitting procedure:

$$Tr(\overline{\overline{p}})^{\mathrm{GSE}} = p_{xx}^{\mathrm{GSE}} + p_{yy}^{\mathrm{GSE}} + p_{zz}^{\mathrm{GSE}} = p_\varphi + p_\psi + p_\eta . \quad (14)$$

In order to obtain the data on the plasma current density inside MCs, we have to calculate the difference between the current densities of the protons and electrons from the data of their corresponding densities and velocities. However, the experimental plasma current density is not too reliable because it is the difference between the components associated with each species, which generally can produce errors in its determination which are bigger than the magnitude of the plasma current density.

On the other hand, we will be interested in the projections of the plasma current densities on the topology of the MC defined by the magnetic field (see the next section). Thus, from Equations (2), (5), and (7) for the magnetic field components, and Equations (9)–(10) for the current density components, we can determine the current density component perpendicular to the magnetic field lines of the MC,

$$|j_\perp| = \frac{|j \times B|}{|B|}, \quad (15)$$

and that parallel to the magnetic topology,

$$j_{||} = \frac{j \cdot B}{|B|}. \quad (16)$$

The perpendicular plasma current density, Equation (15), is expected to involve information similar to the plasma hydrostatic pressure, and thus is related to the expansion of the MC (Hidalgo 2014). However, the parallel plasma current density, Equation (16), provides additional, complementary information about the physical mechanisms associated with the plasma inside MCs. Hence, we incorporate it into our analysis of MCs.

Table 1
MC Time Interval Used in the Analysis of the Events Selected in the Present Work

Event yy-mm-dd	MC Interval (doy)	$\langle v_{\mathrm{SW}} \rangle$ (km s^{-1})
1998 Jan 18	7.183–8.213	390
2000 Jul 26	210.591–211.289	465
2001 Apr 10	102.377–103.297	675
2004 Jan 22	22.519–23.563	575
2004 Nov 14	314.949–315.646	725
2005 May 15	135.464–136.013	820

Note. The corresponding mean velocities, which are necessary in our fitting procedure, are also detailed.

3. DATA

All of the data and experimental information used in the present work come from the ISTP program and OMNIWeb. The cadence of the data used in the present study is five minutes, which were obtained from the *ACE* and *Wind* spacecraft. All of the details can be found in the web page http://omniweb.gsfc.nasa.gov/html/HROdocum.html.

We have noted that the determination of the experimental plasma current density could lead to implicit errors comparable to the current density itself. Instead, we will focus our attention on the parallel component of the proton current density. From Equation (8), we deduce the same behavior for the electron and proton current densities under the conditions fixed in the development of the model. To calculate the corresponding current density for the protons, we will use the data for the magnetic field components from OMNIWeb, in addition to the proton density and velocity.

To establish the boundaries of the selected MCs, we use the plasma beta. In Table 1, we specify the day of year (doy) corresponding to the boundaries of the events analyzed. We also provide the mean velocity of the MC, which is necessary for our fitting procedure.

All of the figures show the following panels: the magnetic field strength, B, the three Cartesian GSE-components (B_x, B_y, B_z), the proton pressure, the parallel proton current density, and the corresponding bulk solar wind velocity. The vertical dotted

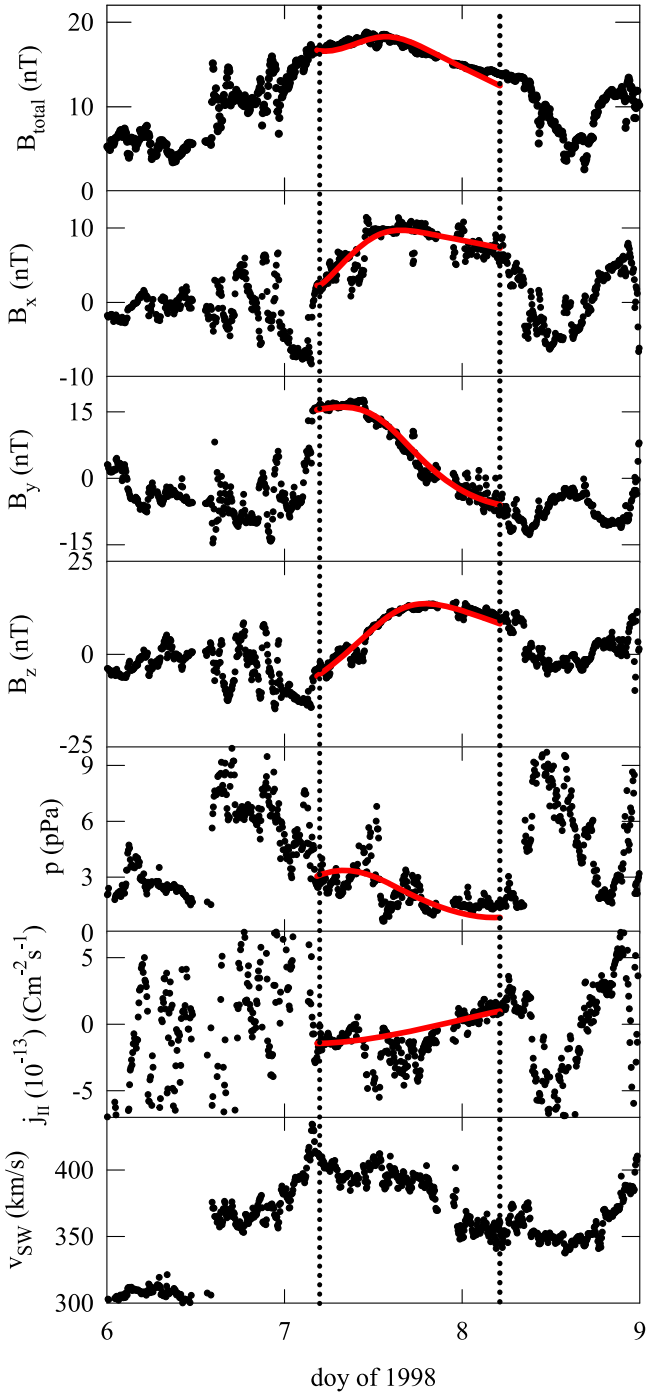

Figure 1. Data obtained from OMNIWeb for the magnetic cloud of 1998 January: the magnetic field strength, B, the Cartesian GSE-components (B_x, B_y, B_z), the proton pressure, and the parallel proton current density. The bulk solar wind velocity is also shown. The vertical dotted lines represent the time boundaries of the cloud as chosen following Burlaga's criteria using the β-plasma. Superimposed on the experimental data are the results of the global model predictions for the different magnitudes as solid lines (see the text for details).

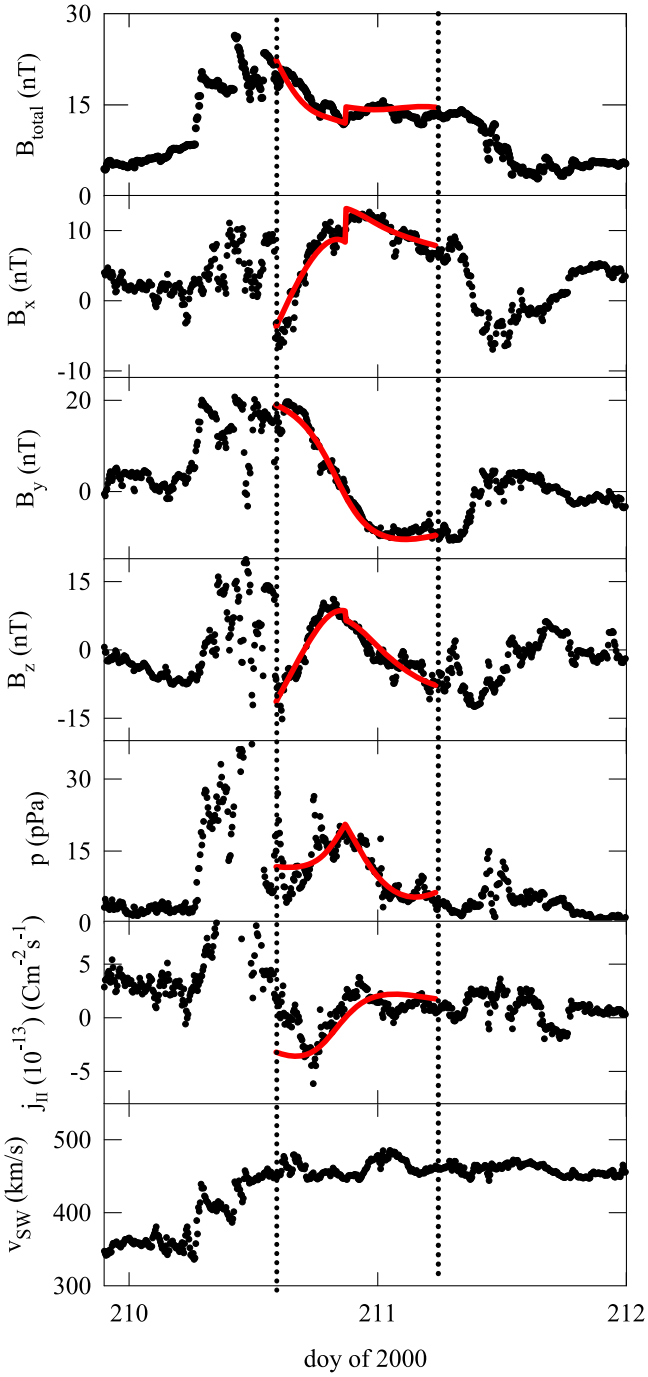

Figure 2. Same graphs as in Figure 1, but for the magnetic cloud of 2000 July.

lines represent the boundaries of the cloud as established from the plasma beta.

We have selected the following six events: 1998 January 18 (Figure 1), 2000 July 26 (Figure 2), 2001 April 10 (Figure 3), 2004 January 22 (Figure 4), 2004 November 14 (Figure 5), and 2005 May 15 (Figure 6).

For 1998 January 18, 2000 July 26, and 2005 May 15, we observe a remarkable feature in the profile of the parallel current density. Its magnitude changes sign when the MC passes the observing spacecraft. This implies a change in the relative sense between the magnetic field and the current density along the structure of the MC. We consider that this is an important point for the understanding of the topology and the physics inside the MCs (see below).

4. PROCEDURE

By taking into account the mean velocity at the interval of every MC, $\langle v_{sw} \rangle$, and the fitting parameters corresponding to

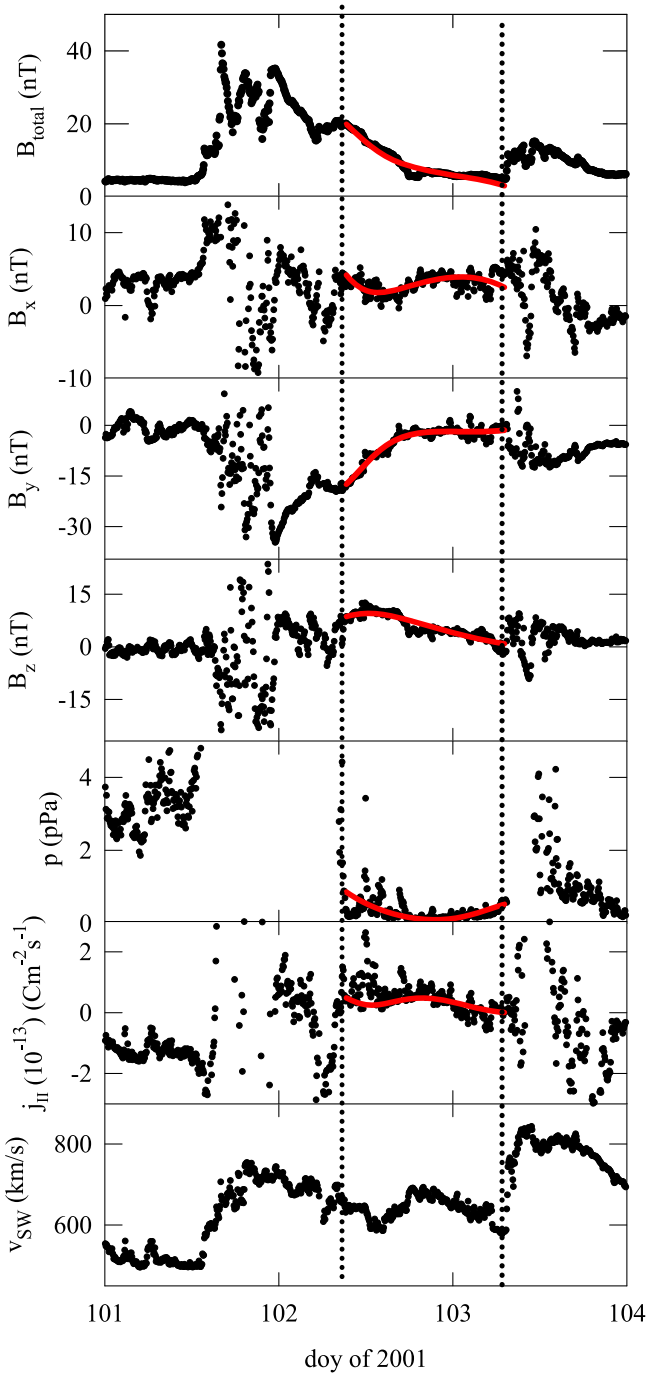

Figure 3. Same graphs as in Figure 1, but for the magnetic cloud of 2001 April.

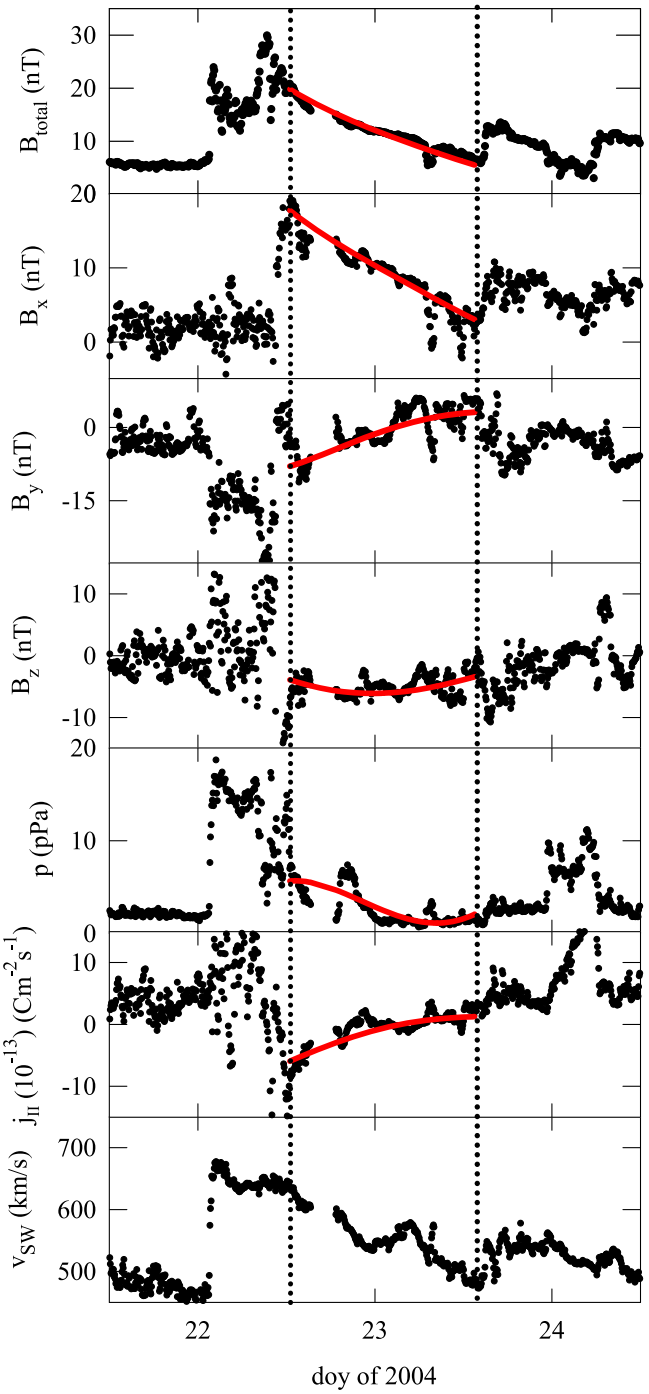

Figure 4. Same graphs as in Figure 1, but for the magnetic cloud of 2004 January.

the orientation of the cloud (the longitude, ϕ, and the latitude, θ, of its axis with respect to the Ecliptic plane, and the minimum distance between the spacecraft path and its axis, y_0), we can determine the theoretical expressions of the local magnetic field components in the GSE coordinate system, the trace of the plasma pressure, and the parallel current density. Additionally, $r_{spc}(t)$, $\phi_{spc}(t)$, and $\psi_{spc}(t)$ are the coordinates of the spacecraft at any time t inside the MC.

Thus, we find that the local magnetic field components in the GSE system are

$$\begin{aligned} B_x^{GSE} &= \cos(\phi)B_x - \sin(\phi)\cos(\theta)B_y + \sin(\phi)\sin(\theta)B_z \\ B_y^{GSE} &= \sin(\phi)B_x + \cos(\phi)\cos(\theta)B_y - \cos(\phi)\sin(\theta)B_z. \\ B_z^{GSE} &= \sin(\theta)B_y + \cos(\theta)B_z \end{aligned} \tag{17}$$

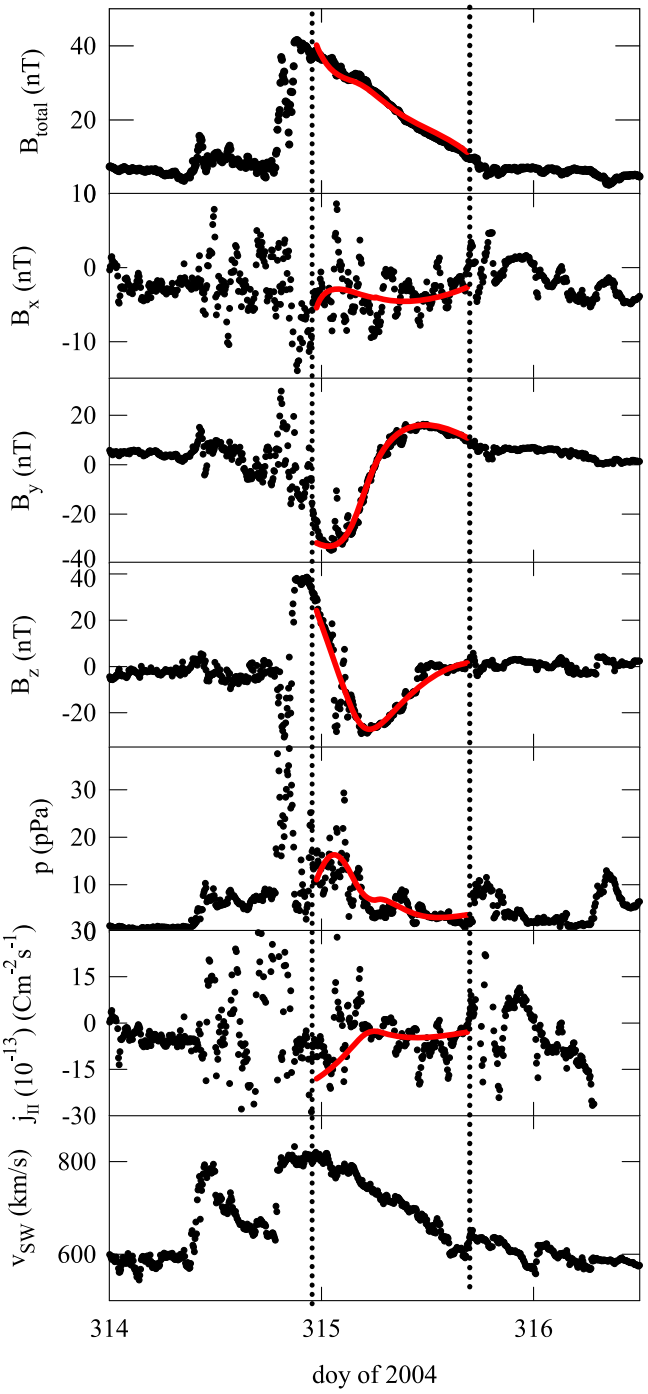

Figure 5. Same graphs as in Figure 1, but for the magnetic cloud of 2004 November.

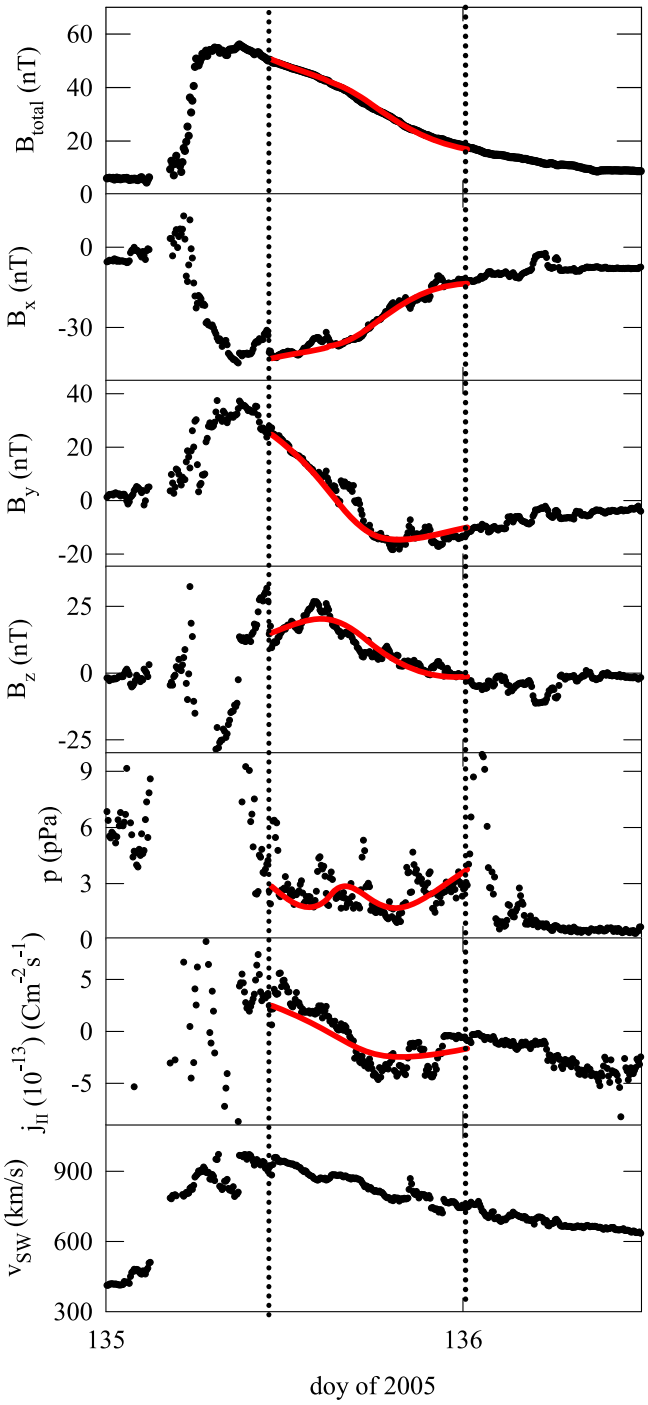

Figure 6. Same graphs as in Figure 1, but for the magnetic cloud of 2005 May.

In Equation (17), the components B_x, B_y, and B_z correspond to the local Cartesian coordinate components of the magnetic field, given by

$$\begin{aligned} B_x &= -\sin(\varphi)\cos(\psi)B_\varphi - \sin(\psi)B_\psi - \cos(\varphi)\cos(\psi)B_\eta \\ B_y &= -\sin(\varphi)\sin(\psi)B_\varphi + \cos(\psi)B_\psi - \cos(\varphi)\sin(\psi)B_\eta \\ B_z &= \cos(\varphi)B_\varphi + \frac{r}{\rho_0}\frac{\partial f(\psi)}{\partial \psi}\sin(\varphi)B_\psi - \sin(\varphi)B_\eta \end{aligned} \quad (18)$$

B_φ, B_ψ, B_η correspond to Equations (2), (5), and (7), respectively.

Introducing the trace of the pressure tensor in the fitting procedure involves one more parameter: the constant parameter related to the pressure, p_0. On the other hand, taking into account the parallel current density in the fitting procedure does not add additional parameters to the fitting procedure. However, the inclusion of this new magnitude allows us to determine the plasma parameters with remarkably fewer dependencies and correlations compared to those obtained when we fit only the magnetic field components.

Even more, because all of the events considered in this paper have been observed around 1 au, we assume a mean radius of

Table 2
MC Parameters Obtained from the Fitting Related to the Axis Orientation, (Latitude, θ, Longitude, ϕ), and the Closet Approach of the Spacecraft to the Axis

Event yy-mm-dd	θ	ϕ^{a}	y_0 (/au)
1998 Jan 18	90	180	0
2000 Jul 26	52	205	0.03
2001 Apr 10	70	255	0.048
2004 Jan 22	128	225	0.053
2004 Nov 14	88	181	0
2005 May 15	78	176	0.001

Note.
[a] Referred to the Sun–Earth line.

the torus, ρ_0, of 0.5 au (for more details see Hidalgo & Nieves-Chinchilla 2012).

Therefore, we simultaneously fit the theoretical GSE magnetic field components, Equation (17), the trace of the pressure tensor, Equation (14), and the parallel current density, Equation (16), to the corresponding data, minimizing the function

$$\chi^2 = \frac{1}{N}\sum [(B^{\rm exp} - B^{\rm GSE})^2 / B_n^2 + ({\rm Tr}(p^{\rm exp}) - {\rm Tr}(p))^2 / p_n^2 + (j_{\parallel}^{\rm exp} - j_{\parallel}^{\rm GSE}) / j_n^2] , \quad (19)$$

where $(B^{\rm exp} - B^{\rm GSE})^2 = (B_{\rm x}^{\rm exp} - B_{\rm x}^{\rm GSE})^2 + (B_{\rm y}^{\rm exp} - B_{\rm y}^{\rm GSE})^2 + (B_{\rm z}^{\rm exp} - B_{\rm z}^{\rm GSE})^2$, with $\boldsymbol{B}^{\rm exp}$ being the experimental magnetic field data in the GSE coordinate systems and $\boldsymbol{B}^{\rm GSE}$ the theoretical magnetic field, Tr(p) being the trace of the hydrostatic pressure, and $j\|$ being the parallel proton current density. N is the number of experimental points to be fit, which is associated with the corresponding data of the MC.

The constants $B_n = 10^{-9}$ T, $p_n = 10^{-12}$ Pa, and $j_n = 10^{-12}\,{\rm C/ms^{-2}}$ have been introduced to provide a dimensionless χ^2 function. Moreover, these factors make every magnitude included in the fitting procedure comparable, so that they are taken at the same level in the optimization of the chi-square function.

In Table 2, we provide the set of MC parameters obtained from the fitting, as well as the axis orientation (latitude, θ, longitude, ϕ) and the closet approach of the spacecraft to the axis. The longitude given refers to the Sun–Earth line. We give only these parameters because they correspond to the parameters available from the other existing MC models.

5. SUMMARY AND DISCUSSION

The two general features of the proposed model are its flux-rope topology and its non-force-free character. Concerning this last assumption, in the figures representing the plasma pressure of all of the MC events analyzed, a non-constant behavior is always observed, which is in contrast to the predictions of the force-free models.

Introducing the behavior of the plasma implies the solution of the force equation (Hidalgo 2014) and the continuity equation (see above), both under the hypothesis and the assumptions of the model. This leads to an improvement of the model, simultaneously fitting the three components of the magnetic field, the plasma pressure, and the parallel current density. No other model in the literature provides the physical information obtained with the model described in the present work.

Important additional information obtained from the model is the rate of expansion of the cross-section of the MC. It assumes, for the sake of physical consistency, a linear time dependence for all of the components of the plasma current density, i.e., proportional to $(t_0 - t)$, where t is the time variable (in our analysis, the time of the passage of the spacecraft through the cloud), and then the same dependence for the magnetic field components and the plasma pressure.

In all of the Figures (1–6), superimposed on the experimental data and averaged over five minutes, are the model predictions, which are represented with solid lines. In light of the theoretical fits, we consider that the obtained results are good, and not only for the magnetic field components but also for the trace of the pressure and the parallel proton current density. This provides us with an important argument to conclude that the global model in the present form can be potentially valuable for the analysis of the magnetic topology of MCs, for their plasma behavior, and their evolution in the interplanetary medium; i.e., the model can help us to understand the physical mechanisms involved in the MCs.

One important (and unexpected) experimental fact observed in several events is the change in the sign of the plasma parallel current density during the passage of the spacecraft through it. This implies a change in the relative sense of the magnetic field vector with respect to the plasma current density vector. Our model includes this behavior, associating its origin with the angular dependence along the cross-section of the MC of the first term of the poloidal component of the magnetic field (Equation (2)).

On the other hand, ICMEs, and in particular MCs, are key drivers of geomagnetic storms (e.g., Gosling 1991; Webb et al. 2000; Leamon et al. 2002, Wu & Lepping 2002, Vieira et al. 2004; Huttunen et al. 2005; Gopalswamy et al. 2015). Because our model seems to be appropriate for the analysis of MCs, it also provides us with a good frame in which to understand their relationship with the associated geomagnetic storms. In fact, in two previous works by the authors, they already used a simpler MC model to develop a preliminary approach to analyze the origin of the geomagnetic storms due to MCs. The authors showed how the orientation of the MCs and the behavior of the plasma inside them could play a crucial role in shaping the geomagnetic storms (Hidalgo 2003; Hidalgo et al. 2005).

The next step will be to include in our analysis the electric field as deduced from the model. However, the main problem with this magnitude is its sensitivity, showing the corresponding spurious data fluctuations, perturbations, and noise due to the influence of, for example, the electrostatic charge of the spacecraft. In fact, we have already made an effort in this direction with our previous elliptical model (Hidalgo 2011), which we expect could guide us in incorporating the electric field into the present global model.

The author acknowledges data and information obtained from the ISTP program, OMNIWeb. This work was supported by the Comisin Interministerial de Ciencia y Tecnología (CICYT) of Spain. Project reference: ESP2013-48346-C2-1-R.

REFERENCES

Burlaga, L. F. 1988, JGR, 93, 7217
Burlaga, L. F., Sittler, E., Mariani, F., & Schwenn, R. 1981, JGR, 86, 6673
Cid, C., Hidalgo, M. A., Nieves-Chinchilla, T., Sequeiros, J., & Viñas, A. F. 2002, SoPh, 207, 187
Goldstein, H. 1983, in NASA Conf. Publ., CP-2280, JPL Solar Wind Five, ed. M. Neugebauer, 731
Gopalswamy, N., Yashiro, S., Xie, H., Akiyama, S., & Mäkëla, P. 2015, JGR, 107, 1142
Gosling, J. T. 1990, in Geophys. Monogr. Vol. 58, ed. E. R. Priest, L. C. Lee, & C. T. Russell, 343
Gosling, J. T. 1991, JGR, 96, 7831
Hidalgo, M. A. 2003, SoPh, 216, 311
Hidalgo, M. A. 2011, JGR, 116, A02101
Hidalgo, M. A. 2013, ApJ, 766, 125
Hidalgo, M. A. 2014, ApJ, 784, 67
Hidalgo, M. A., & Nieves-Chinchilla, T. 2012, ApJ, 748, 109
Hidalgo, M. A., Cantalapiedra, I. R., Sequeiros, J., Cid, C., & Nieves-Chinchilla, T. 2005, AdSpR, 35, 426
Hidalgo, M. A., Nieves-Chinchilla, T., & Blanco, J. J. 2013, SoPh, 284, 151
Hu, Q., & Sonnerup, U. Ö 2002, JGR doi:10.1029/2001JA000293
Huttunen, K. E. J., Schwenn, R., Bothmer, V., & Koskinen, H. E. J. 2005, AnGeo, 23, 625
Jian, L., et al. 2006, SoPh, 239, 393
Kilpua, E. K. J., Isavnin, A., Vourlidas, A., Koskinen, H. E. J., & Rodriguez, L. 2013, AnGeo, 31, 1251
Kilpua, E. K. J., Jian, L. K., Li, Y., Luhmann, J. G., & Russell, C. T. 2011, JASTP, 73, 1228
Leamon, R. J., Canfield, R. C., & Pevtsov, A. A. 2002, JGR, 107(A9), 1234
Lepping, R. P., Burlaga, L. F., Szabo, A., et al. 1997, JGR, 102, 14049
Lundquist, S. 1950, Ark. Fys, 2, 361
Möstl, C., et al. 2009, SoPh, 256, 427
Osherovich, V. A., Farrugia, C. J., & Burlaga, L. F. 1993, AdSpR, 13, 57
Osherovich, V. A., Farrugia, C. J., & Burlaga, L. F. 1995, JGR, 100, 30
Richardson, I. G., & Cane, H. V. 2010, SoPh, 264, 189
Riley, P., & Crooker, N. U. 2004, ApJ, 600, 1035
Riley, P., Linker, J. A., & Mikić, Z. 2001, JGR, 106, 15889
Thernisen, A., Vourlidas, A., & Howard, R. A. 2009, SoPh, 256, 111
Vieira, L. E., et al. 2004, SoPh, 223, 245
Vourlidas, A., Lynch, B. J., Howard, R. A., & Li, Y. 2013, SoPh, 284, 179
Webb, D. F., Cliver, E. W., Crooker, N. U., St. Cyr, O. C., & Thompson, B. J. 2000, JGR, 105, 491
Wu, C. C., & Lepping, R. P. 2002, JGR, 107, 1314